Biointerface Research in Applied Chemistry
Open-Access Journal (ISSN: 2069-5837)

Article
Volume 13, Issue 3, 2023, 275
https://doi.org/10.33263/BRIAC133.275

Theoretical Description for Ibotenic Acid and Muscazone Determination in Mushroom Pulp and Biological Liquids over Conducting Polymer-Modified Electrode

Volodymyr V. Tkach [1,2*], Marta V. Kushnir[1], Vira V. Kopiika [3], Olga V. Luganska[3], Lyudmyla O. Omelyanchik [3], Zholt O. Kormosh [4], Mariia P. Mytchenok [5], Jarem R. Garcia [6], Karina V. Palamarek [7], Konon L. Bagrii [7], Oksana P. Vitriak [8], Anzhelika O. Medvedeva [8], Sílvio C. De Oliveira [2], Petro I. Yagodynets [1,*] Dilafruz B. Razhabova [9], Laziz N. Niyazov [9], Dilfuza M. Musayeva [9], Xayriddin Kosimov [9], Oysha Jabborova [9], Bakhodirjon Samadov [9], Gulandom Sagdullayeva [9], Gulhayo Hamdanova [9], Viktoriia V. Payentko [10], Eugeny M. Demianenko [10], José Inácio Ferrão da Paiva Martins [11], Lucinda Vaz dos Reis [12]

1 Chernivtsi National University, 58000, Kotsyubyns´ky Str. 2, Chernivtsi, Ukraine
2 Federal University of Mato Grosso do Sul, Av. Sen. Felinto. Müller, 1555, C/P. 549, 79074-460, Campo Grande, MS, Brazil
3 Zaporizhzhia National University, 69600, Zhukovsky Str. 66, Zaporizhzhia, Ukraine
4 Eastern European National University, 43000, Voli Ave., 13, Lutsk, Ukraine
5 Bukovinian State Medical University, 58001, Teatralna Sq., 9, Chernivtsi Ukraine
6 State University of Ponta Grossa, Uvaranas Campus, Av. Gal. Carlos Cavalcanti, 4748, 84030-900, Ponta Grossa, PR, Brazil
7 Chernivtsi Institute of Trade and Economics of Kyiv National University of Trade and Economics, 58012, Central Sq. 9, Chernivtsi, Ukraine
8 Kyiv National University of Trade and Economics, 02156, Kyoto Str. 21, Kyiv, Ukraine
9 Abu Ali Ibn Sino Bukhara State Medical Institute, 705018, Navoi Str., 1, Bukhara, Uzbekistan
10 Chuiko Institute of Surface Chemistry of National Academy of Science of Ukraine, 03164, Gen. Naumov Str. 17, Kyiv, Ukraine
11 University of Porto, Engineering Faculty, 4200-465, Rua Dr. Roberto Frias, s/n, Porto, Portugal
12 University of Trás-os-Montes and Alto Douro, Quinta de Prados, 5001-801, Folhadela, Vila Real, Portugal
* Correspondence: nightwatcher2401@gmail.com (V.V.T.); ved1988mid@rambler.ru (P.I.Y.);
Scopus Author ID 55758299100

Received: 27.4.2022; Accepted: 10.06.2022; Published: 10.07.2022

Abstract: The possibility of ibotenic acid and muscazone electrochemical determination, assisted by a conducting polymer electrode, has been developed and evaluated from a theoretical point of view. The correspondent mathematical model has been developed and analyzed by means of linear stability theory and bifurcation analysis. The model analysis has shown that, due to the transformation of the ionic form, the oscillatory behavior in this system tends to be more probable than in similar ones. On the other hand, the electroanalytical system will be efficient for both analytes determination and quantification in mushroom pulp and biological liquids.

Keywords: ibotenic acid; muscazone; electrochemical sensors; electrochemical oscillations; stable steady-state.

1. Introduction

Amanita muscaria, commonly known as fly agaric, is one of the most widespread poisonous mushrooms in moderate and subtropical climatic zones, generally in Europe and

North America [1–4]. Some reports confirm the expansion of its habitat towards tropical, subequatorial, and equatorial countries, like Colombia [4]. Like most of the *Amanita* species, the fly agaric is highly poisonous, the reason why it is not consumed in food, even cooked and roasted.

The main symptoms of mushroom intoxication are [5–8] euphoria, false happiness, vivacity, and hallucinations, followed by sudden depression, anxiety, and slumber. Even in small doses, the detoxification is slow and does not pass by the hangover stage. The high doses may cause irreversible brain damage and behavior changes. The toxic effects of fly agaric are associated with the ibotenic acid and derivatives (Figure 1).

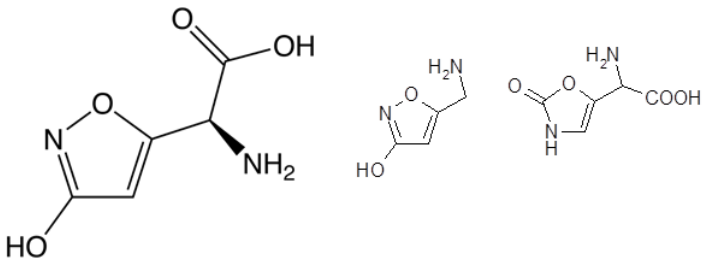

Figure 1. From left to right: ibotenic acid, muscimol and muscazone.

The ibotenic acid (Figure 1. To the left) is the main amino acid of fly agaric. From the chemical point of view, it is a glycine derivative, substituted by an isoxazolic ring, which gives it predominantly basic properties. Its toxicity is based on its facility to trespass the hematoencephalic barrier, to intervene in the synthesis of brain proteins, modifying, directly or indirectly, their composition [9–11]. On the other hand, in some countries, principally in Scandinavian countries, including Iceland, it is still used in popular medicine for brain and spirit stimulation [12]. Moreover, this acid is used in biochemical tests of neurophysiological response[13]. Its decarboxylation converts it into an amine, known as muscimol, an even more poisonous compound (Figure 1. In the middle) [14].

On the other hand, muscazone (Figure 1. To the right) is one of the ibotenic acid isomers produced inside the mushroom by UV-assisted ibotenic acid isomerization. Relating to the ibotenic acid or, even more, to its decarboxylate, muscazone is less toxic [5,14–16] but possesses a somehow more long-time effect and reinforces the toxicity of two other compounds. It provokes memory failure, attention and orientation disorders, and partial vision loss.

Considering the above-cited statements, developing a precise and exact method for determining both amino acids is actual, and the electroanalytical methods could provide a good solution to this problem [17–24].

Some electroanalytical and electrophoretic methods have been developed for the ibotenic acid [17]. As for the muscazone, no electroanalytical method for detecting this amino acid has yet been developed. Considering the presence of highly accepting isoxazolic and oxazolonic rings, the cathodical methods in acidic media are preferable, and the conducting polymers, widely used in electrochemical sensing as active substances and mediators, are widely used in electrochemical sensing could be excellent electrode modifiers for this process [19–24].

Nevertheless, the synthesis and electroanalytical use of the conducting polymers tends to be accompanied by some behavioristic and stability phenomena, like electrochemical oscillations or monotonic behavior [25,26], which may put the practical realization of the

electroanalytical process in jeopardy. A theoretical mechanistic investigation of this process is needed to avoid their realization. Therefore, this work aims to analyze the electroanalytical process of CP-assisted ibotenic acid and muscazone electrochemical determination in terms of mechanism and stability. It also compares its behavior to similar electroanalytical processes [27,28].

2. Materials and Methods

The reduction of the ibotenic acid and muscazone is given by different mechanisms. In both of the cases, the ring cleavage is realized. As for the ibotenic acid, its reduction is realized in two manners. So, schematically, the system's behavior will be realized as in Figure 2.

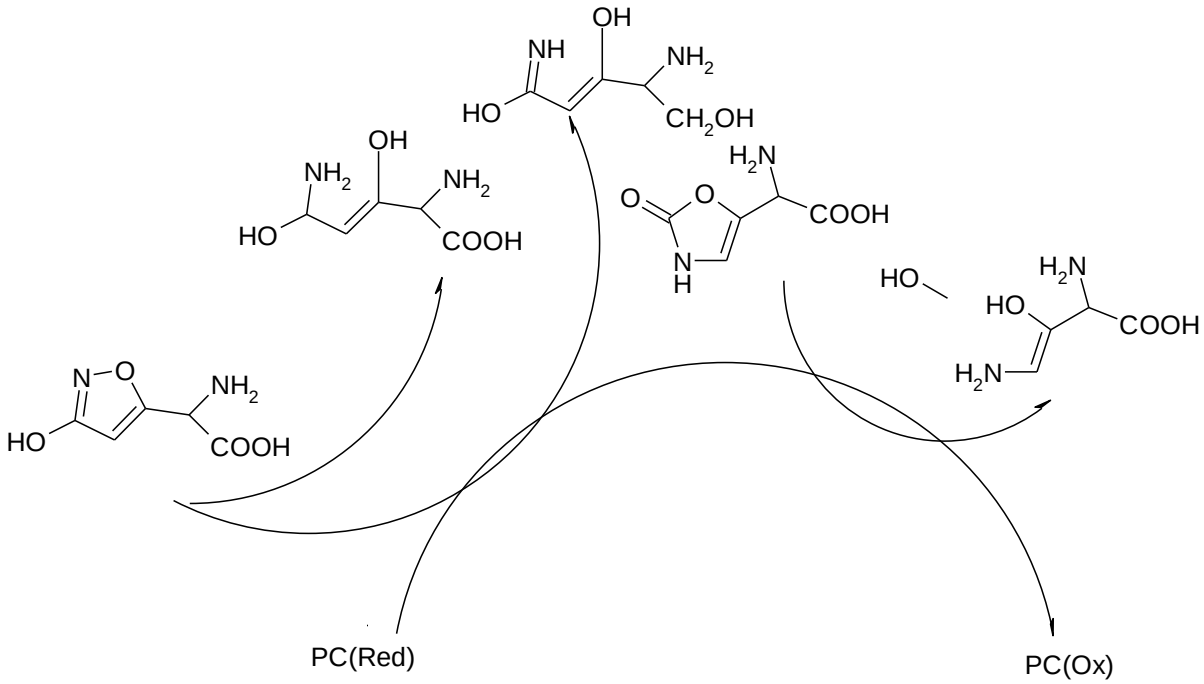

Figure 2. The schematical representation of the electroanalytical process.

It is important to mention that the muscazone electrochemical reduction in the process mimics its metabolism in the human organism. One of the muscazone reduction products is methanol, which is responsible for total or partial blindness, one of the fly agaric intoxication symptoms.

Taking into account the above-cited, to investigate the system's behavior, we introduce three variables:

m – the ibotenic acid concentration in the pre-surface layer;

m* - the muscazone concentration in the pre-surface layer;

p – the oxidized conducting polymer forms surface coverage degree.

Taking into account some assumptions [27–28], we describe the system's behavior by differential equation set (1).

$$\begin{cases} \frac{dm}{dt} = \frac{2}{\delta}\left(\frac{M}{\delta}(m_0 - m) - r_{iso} - r_{11} - r_{12}\right) \\ \frac{dm*}{dt} = \frac{2}{\delta}\left(\frac{M*}{\delta}(m*_0 - m*) + r_{iso} - r_2\right) \\ \frac{dp}{dt} = \frac{1}{P}(r_{11} + r_{12} + r_2 - r_V) \end{cases} \quad (1)$$

Herein, M and M* are the aminoacids diffusion coefficients, m_0 and m^*_0 are the bulk concentrations of each one of the amino acids, P is the oxidized polymer maximal concentrations, and the parameters r are the correspondent reaction rates, calculated as (2–6).

$$r_{iso} = k_{iso} m \exp(-am) \quad (2)$$

$$r_{11} = k_{11} m (1-p)^6 \exp(-am) \quad (3)$$

$$r_{12} = k_{12} m (1-p)^8 \exp(-am) \quad (4)$$

$$r_2 = k_2 m * (1-p)^4 \exp(-bm) \quad (5)$$

$$r_v = k_v p \exp\left(-\frac{nF\varphi_0}{RT}\right) \quad (6)$$

Herein, the parameters k stand for the correspondent rate constants, a and b are the parameters relating the ibotenic acid and muscazone concentrations with the DEL electrochemical and electrophysical parameters, n is the number of the electrons transferred by the polymer on the electrochemical stage, F is the Faraday number, φ_0 is the zero-charge related potential slope, R is the universal gas constant, T is the absolute temperature.

As all of the chemical and electrochemical stages of the process influence the DEL electrochemical and electrophysical properties, the behavior of this system tends to be more dynamic than in similar systems [27,28]. Nevertheless, the electroanalytical efficacy of the process is proven, as shown below.

3. Results and Discussion

In order to investigate the behavior of the CP-assisted ibotenic acid and muscazone electrochemical determination, we analyze the equation-set (1) alongside the algebraic relations (2–6) by means of the linear stability theory. The steady-state Jacobian matrix element values may be expressed as (7).

$$\begin{pmatrix} a_{11} & a_{12} & a_{13} \\ a_{21} & a_{22} & a_{23} \\ a_{31} & a_{32} & a_{33} \end{pmatrix} \quad (7)$$

Herein:

$$a_{11} = \frac{2}{\delta}\Big(-\frac{M}{\delta} - k_{iso}\exp(-am) + ak_{iso}m\exp(-am) - k_{11}(1-v)^6\exp(-am) + ak_{11}m(1-v)^6\exp(-am) - k_{12}(1-v)^8\exp(-am) + ak_{12}(1-v)^8\exp(-am)\Big) \quad (8)$$

$$a_{12} = 0 \quad (9)$$

$$a_{13} = \frac{2}{\delta}(6k_{11}m(1-v)^5\exp(-am) + 8k_{12}m(1-v)^7\exp(-am)) \quad (10)$$

$$a_{21} = \frac{2}{\delta}(k_{iso}\exp(-am)) \quad (11)$$

$$a_{22} = \frac{2}{\delta}\Big(-\frac{M*}{\delta}(m*_0 - m*) - k_2(1-v)^4\exp(-bm) + bk_2 m*(1-v)^4\exp(-bm)\Big) \quad (12)$$

$$a_{23} = \frac{2}{\delta}(4k_2 m*(1-v)^3\exp(-bm)) \quad (13)$$

$$a_{31} = \frac{1}{V}(k_{11}(1-v)^6 \exp(-am) - ak_{11}m(1-v)^6 \exp(-am) + k_{12}(1-v)^8 \exp(-am) - ak_{12}(1-v)^8 \exp(-am)) \quad (14)$$

$$a_{32} = \frac{1}{V}(k_2(1-v)^4 \exp(-bm) - bk_2m * (1-v)^4 \exp(-bm)) \quad (15)$$

$$a_{33} = \frac{1}{V}\left(-6k_{11}m(1-v)^5 \exp(-am) - 8k_{12}m(1-v)^7 \exp(-am) - 4k_2m * (1-v)^3 \exp(-bm) - k_v \exp\left(-\frac{nF\varphi_0}{RT}\right) + jk_v v \exp\left(-\frac{nF\varphi_0}{RT}\right)\right) \quad (16)$$

The oscillatory behavior may be possible if the Hopf bifurcation conditions are satisfied. The necessary condition for its realization is the presence of the positive elements in the Jacobian main diagonal. As is seen by observing the main diagonal elements (8), (12), and (16), the oscillatory behavior in this system is possible. Moreover, it is more probable than in the simplest cases [27,28], as, in the referenced processes, the number of possibly positive elements in the main diagonal is lower.

In this case, the DEL structure is altered during the electrochemical stage and chemical stages, including the isomerization, leading to the ionic form transformation (ibotenate to muscazonate). These structural changes also provoke changes in the values in DEL capacitances, which may cause oscillatory behavior.

This behavior is described by the positivity of the elements $ak_{iso}m \exp(-am) > 0$, $ak_{11}m(1-v)^6 \exp(-am) > 0$ and $ak_{12}(1-v)^8 \exp(-am) > 0$ if a>0, $bk_2m * (1-v)^4 \exp(-bm) > 0$, if b>0 e $jk_v v \exp\left(-\frac{F\varphi_0}{RT}\right) > 0$ if j>0. These elements describe the influences of the DEL capacitances, leading to the oscillatory changes in its conductivity and, therefore, in current. Nevertheless, those instabilities are realized in parameter values beyond the detection limit, as shown below.

To investigate the steady-state stability, we apply the Routh-Hurwitz criterion to the equation-set (1) and rewrite the Jacobian determinant as (17) to avoid the cumbersome expressions:

$$\frac{4}{\delta^2 V}\begin{vmatrix} -\kappa_1 - \Xi - \Lambda & 0 & \Sigma \\ \Xi & -\kappa_2 - X & T \\ \Lambda & X & -\Sigma - T - \Omega \end{vmatrix} \quad (17)$$

Opening the brackets and applying the Det J<0 requisites salient from the criterion, we obtain the steady-state stability condition, exposed as (18):

$$-\kappa_1(\kappa_2\Sigma + X\Sigma + \kappa_2 T + \kappa_2\Omega + X\Omega) - \Xi(\kappa_2\Sigma + \kappa_2 T + \kappa_2\Omega + X\Omega) - \Lambda(\kappa_2 T + \kappa_2\Omega + X\Omega) + \Sigma\kappa_2\Sigma < 0 \quad (18).$$

This condition is written more complex than in [27,28], describing an efficient electroanalytical system, either diffusion or kinetically controlled. In [27,28], the models describe a less dynamic behavior due to the less expressed analytes' influence on the DEL ionic force. In this case, the ionic forms are transformed constantly, providing constant changes in DEL electrophysical and electrochemical properties.

Taking into account that the protons take part directly in the electroanalytical system, lowering the pH will stabilize the system, as it augments the possibility of the conducting polymer to conduct and mediate the proton transfer from the media and the electron transfer from the cathode towards the analytes. Decreasing the pH, the values of the parameters Σ and

T will grow, pushing the left side of the in equation (18) to the more negative values and stabilizing the system. So the steady-state stability will be electroanalytical efficient, corresponding to the linearity of the current – concentration dependence (the model describes the sensor function amperometric mode).

As for the detection limit, its condition is correspondent to the monotonic instability and is described as:

$$-\kappa_1(\kappa_2\Sigma + X\Sigma + \kappa_2 T + \kappa_2\Omega + X\Omega) - \Xi(\kappa_2\Sigma + \kappa_2 T + \kappa_2\Omega + X\Omega) - \Lambda(\kappa_2 T + \kappa_2\Omega + X\Omega) + \Sigma\kappa_2\Sigma = 0 \quad (19).$$

A similar model may also be used in the case of the use of squaraine dyes as electrode modifiers. In this case, the squaraine dye may act either as an active substance or as an electrode mediator and stabilizer for metal-derived nanoparticles due to their conducting polymer-like conjugated system. It may only be accomplished if both squaraine dye forms on the electrode surface are ionic. In this case, one more factor, similar to that observed in [26 – 28], is added, making the system even more dynamic (Figure 3).

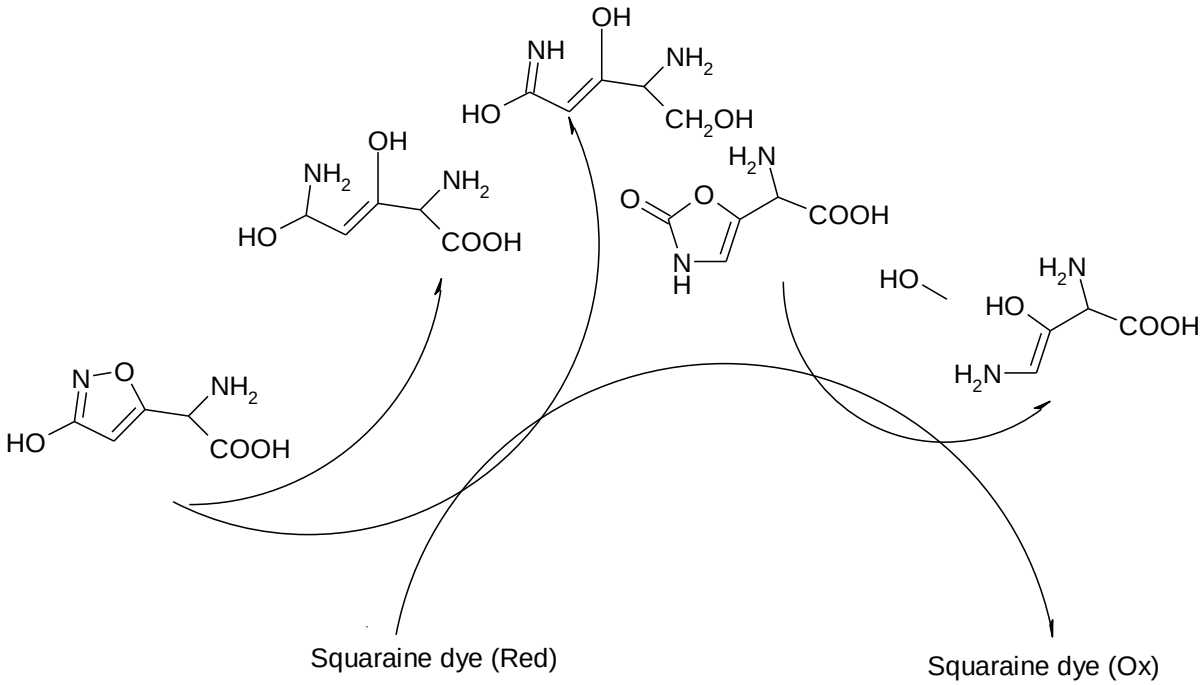

Figure 3. Squaraine-assisted ibotenic acid determination.

Contrarily to ibotenic acid and muscazone, muscimol (Figure 1). The middle may be more efficiently detected electrochemically by an anodic process. In that case, the amino group oxidation will give the principal oxidation mechanism. In our next work, various muscimol electrochemical determination strategies, including cathodic and anodic processes, will be given.

4. Conclusions

The behavior analysis of CP-assisted ibotenic acid and muscazone cathodic electrochemical determination let us conclude that the electroanalytical process is efficient for determining both substances. It is either diffusion or kinetically controlled. The reversibility of the CP electrode is obtained in the electrochemical stage. As for the oscillatory behavior is more probable than in the simplest cases due to the frequent ionic form transformation in DEL.

Funding

This research received no external funding.

Acknowledgments

Volodymyr V. Tkach acknowledges the Engineering Faculty of the University of Porto and the University of Trás-os-Montes and Alto Douro for their support during these difficult times for Ukraine and its research.

Conflicts of Interest

The authors declare no conflict of interest.

References

1. Carboue, Q.; López, M. Amanita muscaria: Ecology, Chemistry, Myths. *Encyclopedia* **2021**, *1*, 905 – 914, https://doi.org/10.3390/encyclopedia1030069.
2. Rampoll, F.I.; Kamler, P; Carlino, C.C.; Bedussi, F. The Deceptive Mushroom: Accidental Amanita muscaria Poisoning. *Eur. J. Case Rep. Int. Med.* **2021,** *8*, 2212, https://doi.org/10.12890/2021_002212.
3. Braeuer, S; Walenta, M; Steiner, L; Goessler, W. Determination of the naturally occurring vanadium complex amavadin in Amanita muscaria with HPLC-ICPMS. *J. Anal. Atom Spectroscop.* **2021,** *36*, 954 – 967, https://doi.org/10.1039/D0JA00518E.
4. Vargas, N; Gonçalves, S.C; Franco-Molano, A.E. *et al.,* In Colombia the Eurasian fungus *Amanita muscaria* is expanding its range into native, tropical *Quercus humboldtii* forests. *Mycologia* **2019,** *111*, 758 – 771, https://doi.org/10.1080/00275514.2019.1636608.
5. Voynova, M; Shkondrov, A; Kondeva-Burdina, M; Krasteva, I. Toxicological and pharmacological profile of Amanita muscaria (L.) Lam. – a new rising opportunity for biomedicine. *Pharmacia* **2020,** *67*, 317 – 323, https://doi.org/10.3897/pharmacia.67.e56112.
6. Gao, J; Xie, R; Wang, N. *et al.* Rapid identification of Amanita citrinoannulata poisoning using colorimetric and real-time fluorescence and loop-mediated isothermal amplification (LAMP) based on the nuclear ITS region. *Food Chem. Mol. Sci.* **2022,** *4*, 100082, https://doi.org/10.1016/j.fochms.2022.100082.
7. Li, S; Liu, K; Liu, Z; Wang, Y. Effect of Four-in-One Optimized Emergency Nursing Procedure on Symptoms and Vital Signs of Patients with Mushroom Poisoning. *J. Healthcare Eng.* **2022,** *2022*, 3387394, https://doi.org/10.1155/2022/3387394.
8. Li, H; Zhang, H.; Zhang, Y. *et al.* Mushroom Poisoning Outbreaks — China, 2019. *China CDC Weekly*, **2020,** *2*, 19, https://doi.org/10.46234/ccdcw2020.005.
9. Sasaki, T.; Hirokatsu, S.; Hiradate, Y. *et al.* Behavioural effects in mice orally exposed to domoic acid or ibotenic acid are influenced by developmental stages and sex differences. *Biochem. Biophys Res. Commun.* **2021,** *558*, 175 – 182, https://doi.org/10.1016/j.bbrc.2021.04.080.
10. Rostampour, M.; Tehrani, B.S.; Babaei, P. Effect of ibotenic acid and colchicine infusion into the rat hippocampus in passive avoidance learning, *Pathobiol. Res.* **2021,** *24*, 37 – 43, https://mjms.modares.ac.ir/article-30-53414-en.html.
11. Modaberi, S; Shahbazi, M.; Naghdi, N; Bagherzadeh, F. Effects of bilateral microinjections of ibotenic acid into neostriatal region and forced exercise on spatial learning and memory and anthropometric characteristics of male rats. *Koomesh* **2021,** *23*, 654 – 664, https://doi.org/10.52547/koomesh.23.5.654.
12. Housecroft, C.E. The fungus *Amanita Muscaria.* From Neutoroxin to Vanadium Accumulation. *Chimia* **2019,** *73*, 96 – 97, https://doi.org/10.2533/chimia.2019.96.
13. Ming, T. Dafny, N. Glutaminergic Signaling in the Nucleus Accumbens Modulates the Behavioral Response to Acute and Chronic Methylphenidate. *J. Exp. Neurol.* **2021,** *2*, 49 – 61, https://www.scientificarchives.com/admin/assets/articles/pdf/glutaminergic-signaling-in-the-nucleus-accumbens-modulates-the-behavioral-response-to-acute-and-chronic-methylphenidate-20210511050554.pdf.

14. Voynova, M; Shkondrov, A; Krasteva, I; Kondeva-Burdina, M. In vitro effects of synthetic muscimol and an extract from Amanita muscaria on human recombinant MAOB enzyme. *Pharmacia*, **2021**, *68*, 147 – 150, https://doi.org/10.3897/pharmacia.68.e60705.
15. Lee, S.; Yu, Y.S; Lee, S.R.; Kim, K.H. Non-peptide secondary metabolites from poisonous mushrooms: overview of chemistry, bioactivity, and biosynthesis. *Nat. Prod. Rep.* **2022,** *39*, 512 – 559, https://doi.org/10.1039/D1NP00049G.
16. Obermaier, S; Müller, M. Ibotenic Acid Biosynthesis in the Fly Agaric is Initiated by Glutamate Hydroxylation. *Angew. Chem. Int. Ed.* **2020,** *59*, 12432 – 12435, https://doi.org/10.1002/anie.202001870.
17. Poliwoda, A; Zielinska, K; Halama, M; Wieczorek, P. Determination of muscimol and ibotenic acid in mushrooms of Amanitaceae by capillary electrophoresis. *Electrophoresis* **2014,** *35*, 2593, http://dx.doi.org/10.1002/elps.201400104.
18. Mule, S; Pansare, D; Gore, V.A. *et al.* A Facile One-Pot Synthesis of 1,4-Dihydropyridine Derivative by Using Polyaniline Supported Zinc Oxide Nanoparticle via Hantzsch Reaction. *Lett. Appl. NanoBioSci.* **2023,** *12*, 17, https://doi.org/10.33263/LIANBS121.017.
19. Joshi, N.C.; Malik, S.; Gururani, P. Utilization of Polypyrrole/ZnO Nanocomposite in the Adsorptive Removal of Cu^{2+}, Pb^{2+} and Cd^{2+} Ions from Wastewater. *Letters in Applied NanoBioScience* **2021**, *10*, 2339–2351, https://doi.org/10.33263/LIANBS103.23392351.
20. de Oliveira, R.W.S.; Barros Gomes, P.R.; Diniz Ribeiro, J. *et al.* Determinação Espectrofotométrica de Cobre (II) em Aguardente de Mandioca (Tiquira). *Rev. Colomb. Cien. Quím. Farm.* **2020**, *49*, 353 – 371, https://doi.org/10.15446/rcciquifa.v49n2.89507 (in Portuguese).
21. Akkapinyo, Ch.; Subannajui, K; Poo-Arporn, Y.; Poo-Arporn, R. P. Disposable Electrochemical Sensor for Food Colorants Detection by Reduced Graphene Oxide and Methionine Film Modified Screen Printed Carbon Electrode. *Molecules* **2021,** *26*, 2312, https://doi.org/10.3390/molecules26082312.
22. Monnappa, A.B.; Manjunatha, J.G.G.; Bhatt, A.S.; Nagarajappa, H. Sensitive and Selective Electrochemical Detection of Vanillin at Graphene Based Poly(Methyl Orange) Modified Paste Electrode. *J. Sci. Adv. Mat. Dev.* **2021,** https://doi.org/10.1016/j.jsamd.2021.05.002.
23. Thadathil, A.; Pradeep, H.; Joshy, D. *et al.*, Polyindole and Polypyrrole as a Sustainable Platform for Environmental Remediation and Sensor Applications. *Mater Adv.* **2022,** *3*, 2990 – 3022, https://doi.org/10.1039/D2MA00022A.
24. Ramanavicius, S.; Morkvenaite-Vilkonciene, I; Samukaite-Bubniene, U. *et al.* Electrochemically Deposited Molecularly Imprinted Polymer-Based Sensors. *Sensors* **2022,** *22*, 1282, https://doi.org/10.3390/s22031282.
25. Das, I.; Goel, N.; Agrawal, N.R.; Gupta, S.K. Growth Patterns of Dendrimers and Electric Potential Oscillations during Electropolymerization of Pyrrole using Mono- and Mixed Surfactants. *The Journal of Physical Chemistry B* **2010**, *114*, 12888-12896, https://doi.org/10.1021/jp105183q.
26. Das, I.; Goel, N.; Gupta, S.K.; Agrawal, N.R. Electropolymerization of pyrrole: Dendrimers, nano-sized patterns and oscillations in potential in presence of aromatic and aliphatic surfactants. *Journal of Electroanalytical Chemistry* **2012**, *670*, 1-10, https://doi.org/10.1016/j.jelechem.2012.01.023.
27. Tkach, V.; Kushnir, M.; de Oliveira, S.; Salomova, H.; Jalilov, F.; Jalilova, F.; Musayeva, D.; Niyazov, L.; Ivanushko, Y.; Ahafonova, O.; Mytchenok, M.; Yagodynets´, P.; Kormosh, Z.; Reis, L.; Palytsia, Y. The Theoretical Description for Fluoxetine Electrochemical Determination, Assisted by CoO(OH)-Nanoparticles, Deposited Over the Squaraine Dye. *Orbital - The Electronic Journal of Chemistry* **2021**, *13*, 53-57, https://doi.org/10.17807/orbital.v13i1.1573.
28. Tkach, V.; Kushnir, M.; de Oliveira, S.; Ivanushko, Y.; Tkach, V.; Mytrofanova, H.; Zadoia, A.; Yagodynets', P.; Kormosh, Z.; Luganska, O. Theoretical Description for an Efficient Rhenium Electrocatalytical Recuperation by Polypyrrole Overoxidation. *Letters in Applied NanoBioScience* **2021**, *10*, 2396-2401, https://doi.org/10.33263/LIANBS103.23962401.